Applied Physics Letters

Electroluminescence of hot electrons in AlGaN/GaN high-electron-mobility transistors under radio frequency operation

Cite as: Appl. Phys. Lett. **106**, 213502 (2015); https://doi.org/10.1063/1.4921848
Submitted: 17 March 2015 . Accepted: 16 May 2015 . Published Online: 26 May 2015

Tommaso Brazzini, Michael A. Casbon, Huarui Sun, Michael J. Uren, Jonathan Lees, Paul J. Tasker, Helmut Jung, Hervé Blanck, and Martin Kuball

ARTICLES YOU MAY BE INTERESTED IN

Progressive failure site generation in AlGaN/GaN high electron mobility transistors under OFF-state stress: Weibull statistics and temperature dependence
Applied Physics Letters **106**, 043505 (2015); https://doi.org/10.1063/1.4907261

Degradation of AlGaN/GaN high electron mobility transistors related to hot electrons
Applied Physics Letters **100**, 233508 (2012); https://doi.org/10.1063/1.4723848

Polarization effects, surface states, and the source of electrons in AlGaN/GaN heterostructure field effect transistors
Applied Physics Letters **77**, 250 (2000); https://doi.org/10.1063/1.126940

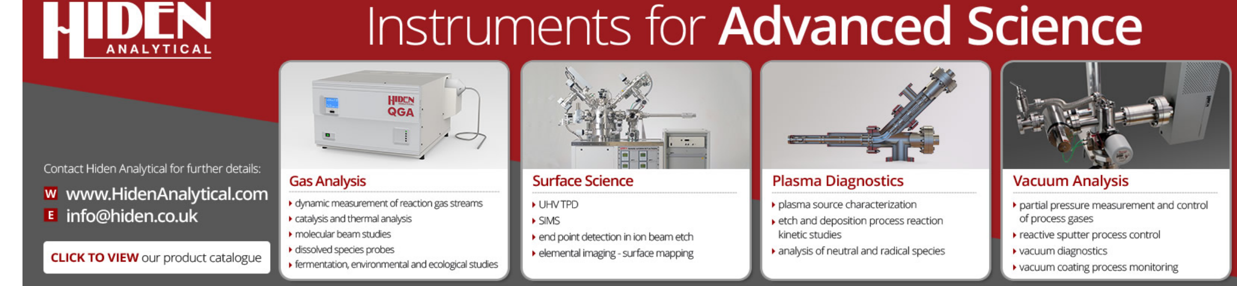

© 2015 AIP Publishing LLC.

APPLIED PHYSICS LETTERS **106**, 213502 (2015)

Electroluminescence of hot electrons in AlGaN/GaN high-electron-mobility transistors under radio frequency operation

Tommaso Brazzini,[1,a)] Michael A. Casbon,[2] Huarui Sun,[1] Michael J. Uren,[1] Jonathan Lees,[2] Paul J. Tasker,[2] Helmut Jung,[3] Hervé Blanck,[3] and Martin Kuball[1]

[1]*Center for Device Thermography and Reliability, H. H. Wills Physics Laboratory, University of Bristol, Bristol BS8 1TL, United Kingdom*

[2]*Centre for High Frequency Engineering, Cardiff University, Cardiff CF24 3QR, United Kingdom*

[3]*United Monolithic Semiconductors GmbH, Wilhelm-Runge-Strasse 11, 89081 Ulm, Germany*

(Received 17 March 2015; accepted 16 May 2015; published online 26 May 2015)

Hot electrons in AlGaN/GaN high electron mobility transistors are studied during radio frequency (RF) and DC operation by means of electroluminescence (EL) microscopy and spectroscopy. The measured EL intensity is decreased under RF operation compared to DC at the same average current, indicating a lower hot electron density. This is explained by averaging the DC EL intensity over the measured load line used in RF measurements, giving reasonable agreement. In addition, the hot electron temperature is lower by up to 15% under RF compared to DC, again at least partially explainable by the weighted averaging along the specific load line. However, peak electron temperature under RF occurs at high V_{DS} and low I_{DS} where EL is insignificant suggesting that any wear-out differences between RF and DC stress of the devices will depend on the balance between hot-carrier and field driven degradation mechanisms. © *2015 AIP Publishing LLC.*
[http://dx.doi.org/10.1063/1.4921848]

AlGaN/GaN electronic devices have been recognized as very promising for applications in the field of radio frequency (RF) amplification as well as power switching. Despite extensive studies on DC-related device degradation and lifetime testing,[1] limited attention has been paid to RF induced device wear-out. In order to overcome RF life test complexity, the DC counterpart is generally used.[2] However, the comparison between DC and RF stress is always a matter of debate.[2–5] According to Joh and Del Alamo,[3] RF stress degrades the device more severely than DC stress at the same bias point, and this effect increases with input power. The degradation has been attributed to trap formation due to hot carriers. Generation of traps with 0.5 eV activation energy, both due to DC and RF, has been reported by Chini *et al.*,[4] likewise with more severe degradation observed under RF. However, data also exist that suggest the device degradation may actually be no worse or even less under RF operation, compared to DC stressing as, for example, observed by Caesar *et al.*[5] Hence, it is essential to identify the microscopic processes involved in the conduction and degradation mechanisms of high electron mobility transistors (HEMTs) under DC and RF conditions, in particular, the hot electron behavior, to justify any DC life test developed for RF reliability assessment. Electroluminescence (EL) has been used as a tool to monitor hot carriers under DC operation.[1,6] It has been suggested that the amount of device degradation is correlated to the EL intensity, which would in this case indicate degradation due to hot electrons to be the dominant mechanism.[7,8] However, EL characteristics of AlGaN/GaN HEMTs during RF operation have not been investigated so far. In this letter, we characterize hot electron effects during device RF operation by means of EL microscopy and spectroscopy. It is demonstrated that hot carrier density and temperature under RF operation are, on average, significantly less in RF than under DC device operation. However, it is also shown that the highest electron temperature occurs under conditions where EL intensity is insignificant suggesting that EL is not necessarily a reliable indicator of device wear-out.

The $4 \times 100\,\mu$m HEMT studied here consist of an AlGaN/GaN heterostructure with a Fe-doped GaN buffer layer on a semi-insulating SiC substrate, with a 0.25 μm gate length and source connected field plate. During testing under RF excitation, the device was operated in class B using a passive matching section circuit, built following active load-pull characterization. This is a practical and compact solution for RF amplification integrated with optical benches (microscopy and spectroscopy). Class B operation is frequently employed in RF power amplifier stages since it delivers high power added efficiency. It involves applying a resistive load at the fundamental frequency and a short circuit at the second harmonic. The result is a nominally sinusoidal drain voltage and a half wave rectified current waveform, which flows primarily when the voltage is at a minimum, thus minimizing dissipation and maximizing efficiency. A 1 GHz signal was applied to the gate of the device using a vector network analyzer (VNA). The dynamic current-voltage locus was varied by changing the input RF power. While the correct fundamental load could be realized, the inevitable losses in the passive tuner meant that a reflection coefficient of 0.8 (64% reflection) was present at the second harmonic.

EL intensity measurements of light emitted from the AlGaN/GaN HEMTs were performed using an optical microscope with a 50× objective and a Hamamatsu digital

[a)]Author to whom correspondence should be addressed. Electronic mail: tommaso.brazzini@bristol.ac.uk

 © 2015 AIP Publishing LLC

CCD camera, while optical spectra from EL emission were obtained using a Renishaw InVia spectrometer. Micro-Raman thermography was used to determine device temperature with more details on the technique given in Ref. 9. Raman and EL measurements were performed from the back side of the device through the transparent GaN layer and SiC substrate, enabling access to the entire source-drain region including areas underneath the metal contacts.

Fig. 1 displays a contour map of EL intensity in the I_{DS}-V_{DS} plane, determined under DC bias conditions. The highest EL signal occurs in the semi-on region, where the product of drain current and electric field in the channel is maximum. This is in agreement with earlier reported data.[1] The EL intensity decreases to zero or negligible values in the pinch-off region ($I_{DS} \leq 10\,\text{mA}$) and in the linear region ($V_{DS} < V_{sat}$). The EL intensity, normalized with the I_{DS}, is expected to follow an exponential law with the inverse of the electric field in the channel given by[1]

$$\frac{I_{EL}}{I_{DS}} \sim \exp\left(-\frac{A}{V_{DS} - V_{sat}}\right), \qquad (1)$$

where I_{EL} is the EL intensity, I_{DS} is the drain current, V_{DS} is the drain voltage, V_{sat} is the current-saturation voltage, and A is a proportionality constant. Fig. 1 also shows the dynamic current-voltage trajectory (load lines) of the device studied under RF, taken with an active load-pull system at different input drive levels and including their corresponding average DC drain current. Under DC operation, a load line was used with a resistance (R_L) of 125 Ω. This value has been selected to track the on-part of the RF load-line dynamic behavior (as shown in Fig. 1). In that way, a valid comparison between RF and DC experiment is possible.

The EL intensity as a function of the average drain current under RF is compared to the results under DC in Fig. 2. For RF excitation, the quiescent bias point was set to $V_{DS} = 24$ V and $V_{GS} = -3.7$ V and the RF input power was varied between −10 and 15 dBm. Clearly apparent is a decreased EL intensity measured under RF compared to that measured under DC.

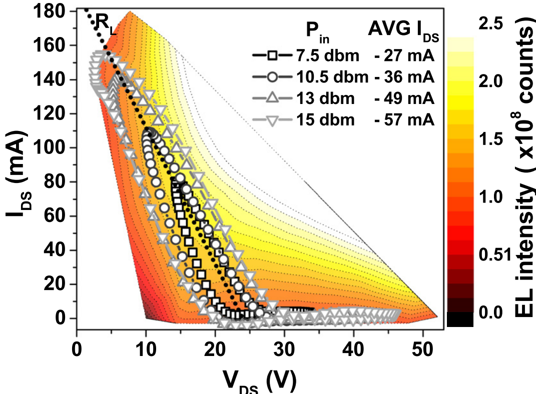

FIG. 1. Contour map of the EL intensity of an AlGaN/GaN HEMT as a function of drain voltage and drain current obtained under DC operation. Superimposed are the load lines for class B for the indicated input powers (P_{in}) and average drain current (AVG I_{DS}). The quiescent bias point is located at $V_{DS} = 24$ V and $V_{GS} = -3.7$ V. The black dotted line represents the load line used for the DC EL intensity measurements with load resistance R_L.

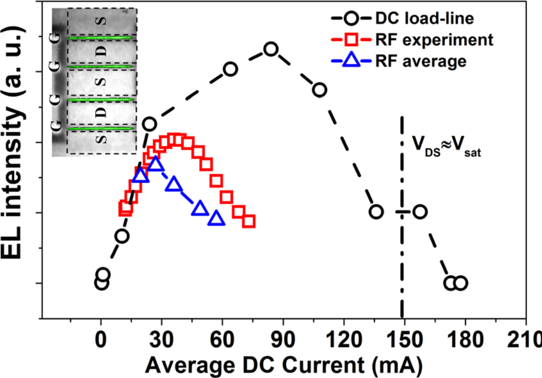

FIG. 2. Electroluminescence (EL) intensity from an AlGaN/GaN HEMT as a function of average DC drain current for RF class B and DC operations, and the intensity integrated over the RF load line. The dashed lines are a guide to the eye. The vertical dashed-dotted line indicates where the current saturation onset starts (i.e., $V_{DS} \approx V_{sat}$). In the inset, the false color EL image is overlaid on a white-light image from the 4 × 100 μm-wide device.

Knowing the RF load line allows the reduced EL intensity under RF to be understood by comparison with the EL intensity at static DC points along this load line. This is shown in Fig. 3(b) with indices corresponding to 62.5 ps intervals during the 1 ns cycle defined in Fig. 3(a). The highest EL intensity occurs in the semi-on region of the I_{DS}-V_{DS} plane. By averaging over the 16 points, the average EL intensity measured for each load line is obtained. This "RF average" value is displayed in Fig. 2, for each P_{in} (or average DC current value), and compared to the EL intensity measured under RF. Very reasonable agreement is obtained; the small differences are presumably due to effects such as self-heating which is greater under "RF average" than under the actual RF experiment, inducing a reduction in the overall EL intensity measured, as already observed previously.[10] The results highlight that under RF there is a lower hot-electron concentration, on average, than under DC. This is a consequence of the time averaging of signal on different part of the I_{DS}-V_{DS} plane, where the most important hot-carrier contribution comes from the semi-on part. This fact is important for the evaluation of the effect of stressing on the reliability of AlGaN/GaN HEMTs, since hot electrons have always been identified as one source of device degradation and failure.[7]

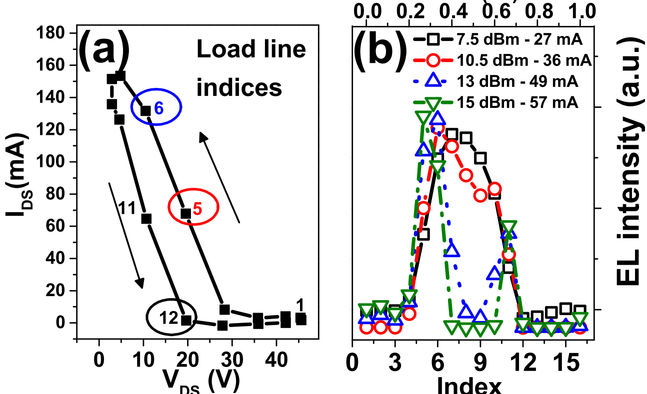

FIG. 3. (a) Load line for class B RF operation used, indicating points used for the detailed analysis of the EL intensity and EL spectrum. Only the 15 dBm load line is shown for clarity. (b) EL intensity versus index on the load line, over a full RF cycle. On the top x-axis the time scale is shown.

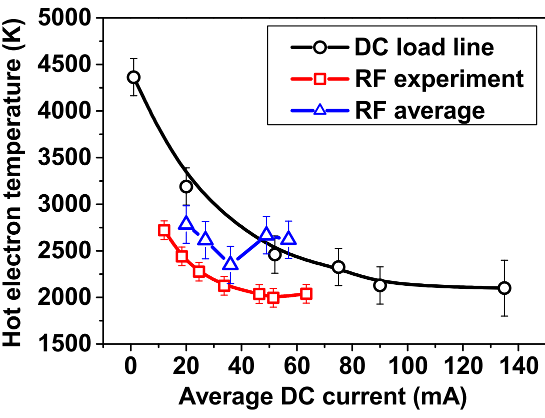

FIG. 4. Electron temperature obtained on an AlGaN/GaN HEMT operated under RF and DC as a function of average drain current determined by the EL spectrum. The curves are a guide for the eye.

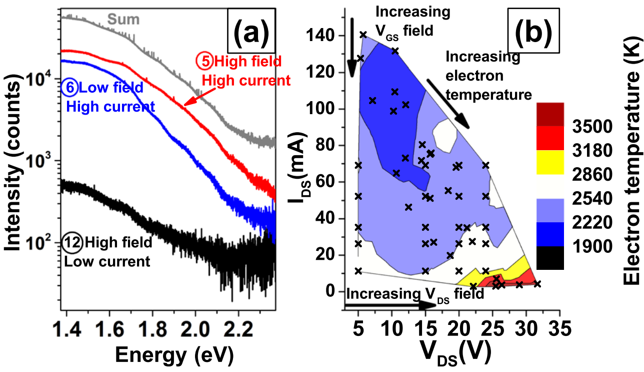

FIG. 5. (a) Spectra of three representative points of the 15 dBm class B load line with index numbers shown in Fig. 3(a) and the spectrum obtained as a sum of all the spectra over all the indices. (b) Electron temperature contour map in the I_{DS}-V_{DS} plane measured under DC conditions. The crosses represent the points of measurement.

However, electron temperature is also a key parameter since above a certain energy threshold, hot carriers can modify point defects in the AlGaN or GaN.[11] Hence, to gain further insight into the difference between RF and DC operation, the energy distribution of hot electrons has been investigated through EL spectroscopy. In fact, spectrally resolved EL emission is known to follow a Maxwell-Boltzmann distribution which, in the high energy part of the spectrum, can be approximated by an exponential function of the following form:[1]

$$EL(E_{h\nu}) \sim \exp\left(-\frac{E_{h\nu}}{k_B(T_{el} - T_{latt})}\right), \tag{2}$$

with photon energy $E_{h\nu}$, electron temperature T_{el}, lattice temperature T_{latt}, and k_B the Boltzmann constant. For higher electric fields in the channel, a higher electron temperature is anticipated. The lattice temperature rise under the operating conditions was estimated with Raman thermography to be at most 30 °C in the range of currents used in the experiment and was insignificant compared to the electron temperature. The effect of lattice temperature increase was taken into account by the T_{latt} term, hence the outcomes of the experiment were less affected by self-heating, unlike the intensity measurements

Figure 4 compares the electron temperature extracted under RF operation to DC. The values obtained under RF are significantly lower than under DC conditions by at most 500 K at the same average current, consistent with the reduced EL intensity under RF of Figure 2. To better understand the spectral measurements, similar to the intensity measurements, an average hot-electron temperature under RF was extracted using the DC bias points along the measured RF load line and added to Figure 4. This also produced an "RF average" electron temperature lower than the DC value, but not as low as the RF experiment. This averaging process has a strong weighting towards the highest intensity contribution as can be inferred from the spectra in Figure 5(a). Averaging the EL spectra along the RF load line is dominated by the spectrum under semi-on conditions due to its high intensity (Fig. 5(a) with index 5 in Fig. 3(a)). The comparison between "RF average" and RF experimental shows a reduction of the electron temperature due to a reduction of the effective electric field in the device under RF. The main reason for that is thought to be the charge trapping under RF, either in the buffer[12] or on the surface[13,14] (virtual gate), responsible for current collapse during high frequency operation. The effect is substantially a smear-out of the electric field under RF, i.e., a reduction of the effective electric field and therefore of the hot carrier temperature.

To consider the implications of the results obtained here for device reliability, i.e., RF versus DC lifetime testing, it is important to realize that the RF experimental EL data are effectively averaged values, but there are peaks in hot carrier density and temperature at certain times in the RF load line. In particular, the high V_{DS} and low I_{DS} (high negative V_{GS}) part of the I_{DS}-V_{DS} plane does not contribute significantly to the EL intensity (see Fig. 1) and spectrum (as shown in Figure 5(a)), but it does result in carriers with high electron temperature. This is apparent in the electron temperature map in Figure 5(b). The density of these very hot carriers may be small, however these are carriers with much higher energy than under DC, and pure electric field induced device degradation contributes here as well.[15–17] This part of the RF load line will ultimately determine whether RF stress results in faster or slower device degradation. Only if this region is not dominant will RF stress result in lower device degradation than under DC due to the smaller average hot carrier density and energy.

In conclusion, hot-electron concentration and temperature during RF operation in class B in AlGaN/GaN HEMTs were compared with DC conditions using EL intensity and spectrum measurements. The results showed that hot electron density under RF operation along a class B load line is lower, on average, than under DC operation, obtained on a load line with the same load resistance. The results suggest that degradation under RF compared to DC should be reduced, but only if field-driven degradation at high V_{DS} is insignificant. The corollary is that electroluminescence is only a good reliability indicator if field driven mechanisms can be excluded.

This work was supported by the UK Engineering and Physical Sciences Research Council (EPSRC) under Grant Nos. EP/K026232 and EP/K02633X. We thank J. W. Pomeroy, A. Sarua, and J. Anaya Calvo for Raman measurements and discussions.

[1]G. Meneghesso, G. Verzellesi, F. Danesin, F. Rampazzo, F. Zanon, A. Tazzoli, M. Meneghini, and E. Zanoni, IEEE Trans. Device Mater. Reliab. **8**, 332 (2008).
[2]J. Joh, J. A. Del Alamo, U. Chowdhury, and J. L. Jimenez, in *ROCS Workshop, Reliability of Compound Semiconductors Workshop*, Monterey, California, 12 October 2008, edited by P. Ersland and K. McGhee (2008), pp. 185–194.
[3]J. Joh and J. A. Del Alamo, IEDM Tech. Dig. **2010**, 20.2.1.
[4]A. Chini, F. Fantini, V. Di Lecce, M. Esposto, A. Stocco, N. Ronchi, F. Zanon, G. Meneghesso, and E. Zanoni, IEDM Tech. Dig. **2009**, 1.
[5]M. Caesar, M. Dammann, V. Polyakov, P. Waltereit, W. Bronner, M. Baeumler, R. Quay, M. Mikulla, and O. Ambacher, IEEE IRPS **2012**, CD.6.1.
[6]H. Sun, M. Montes Bajo, M. J. Uren, and M. Kuball, Microelectron. Reliab. **54**, 2650 (2014).
[7]M. Meneghini, A. Stocco, R. Silvestri, G. Meneghesso, and E. Zanoni, Appl. Phys. Lett. **100**, 233508 (2012).
[8]M. Meneghini, G. Meneghesso, and E. Zanoni, IEEE Trans. Device Mater. Reliab. **13**, 357 (2013).
[9]J. W. Pomeroy, M. Kuball, D. J. Wallis, A. M. Keir, K. P. Hilton, R. S. Balmer, M. J. Uren, T. Martin, and P. J. Heard, Appl. Phys. Lett. **87**, 103508 (2005).
[10]N. Shigekawa, K. Shiojima, and T. Suemitsu, J. Appl. Phys. **92**, 531 (2002).
[11]Y. S. Puzyrev, B. R. Tuttle, R. D. Schrimpf, D. M. Fleetwood, and S. T. Pantelides, Appl. Phys. Lett. **96**, 053505 (2010).
[12]M. J. Uren, J. Möreke, and M. Kuball, IEEE Trans. Electron Devices **59**, 3327 (2012).
[13]R. Vetury, R. Zhang, N. Q. Keller, and U. K. Mishra, IEEE Trans. Electron Devices **48**, 560 (2001).
[14]C. Roff, J. Benedikt, P. J. Tasker, D. J. Wallis, K. P. Hilton, J. O. Maclean, D. G. Hayes, M. J. Uren, and T. Martin, IEEE Trans. Electron Devices **56**, 13 (2009).
[15]M. Montes Bajo, H. Sun, M. J. Uren, and M. Kuball, Appl. Phys. Lett. **104**, 223506 (2014).
[16]P. Makaram, J. Joh, J. A. del Alamo, T. Palacios, and C. V. Thompson, Appl. Phys. Lett. **96**, 233509 (2010).
[17]H. Sun, M. Montes Bajo, M. J. Uren, and M. Kuball, Appl. Phys. Lett. **106**, 043505 (2015).